

Article

Detecting Heavy Neutral SUSY Higgs Bosons Decaying to Sparticles at the High-Luminosity LHC

Howard Baer ^{1,2,*} , Vernon Barger ², Xerxes Tata ³ and Kairui Zhang ²¹ Homer L. Dodge Department of Physics and Astronomy, University of Oklahoma, Norman, OK 73019, USA² Department of Physics, University of Wisconsin, Madison, WI 53706, USA³ Department of Physics and Astronomy, University of Hawaii, Honolulu, HI 53706, USA

* Correspondence: baer@ou.edu

Abstract: In supersymmetry (SUSY) models with low electroweak naturalness (natSUSY), which have been suggested to be the most likely version of SUSY to emerge from the string landscape, higgsinos are expected at the few hundred GeV scale, whilst electroweak gauginos inhabit the TeV scale. For TeV-scale heavy neutral SUSY Higgs bosons H and A , as currently required by LHC searches, the dominant decay modes of H , A are gaugino plus higgsino provided these decays are kinematically open. The light higgsinos decay to soft particles, so are largely invisible, whilst the gauginos decay to W , Z or h plus missing transverse energy (E_T). Thus, we examine the viability of H , $A \rightarrow W + E_T$, $Z + E_T$ and $h + E_T$ signatures at the high luminosity LHC (HL-LHC) in light of large standard model (SM) backgrounds from (mainly) $t\bar{t}$, VV and Vh production (where $V = W, Z$). We also examine whether these signal channels can be enhanced over backgrounds by requiring the presence of an additional soft lepton from the decays of the light higgsinos. We find significant regions in the vicinity of $m_A \sim 1\text{--}2$ TeV of the m_A vs. $\tan\beta$ plane, which can be probed at the high luminosity LHC, using these dominant signatures by HL-LHC at 5σ and at the 95% confidence level (CL).

Keywords: Higgs bosons; LHC; supersymmetry; naturalness

Citation: Baer, H.; Barger, V.; Tata, X.; Zhang, K. Detecting Heavy Neutral SUSY Higgs Bosons Decaying to Sparticles at the High-Luminosity LHC. *Symmetry* **2023**, *15*, 548. <https://doi.org/10.3390/sym15020548>

Academic Editors: Tianjun Li and Jun-Jie Cao

Received: 26 January 2023

Revised: 9 February 2023

Accepted: 15 February 2023

Published: 18 February 2023



Copyright: © 2023 by the authors. Licensee MDPI, Basel, Switzerland. This article is an open access article distributed under the terms and conditions of the Creative Commons Attribution (CC BY) license (<https://creativecommons.org/licenses/by/4.0/>).

1. Introduction

An advantage to searching for (R-parity conserving) supersymmetry [1–3] (SUSY) via heavy Higgs boson production at the CERN Large Hadron Collider (LHC) is that, instead of having to pair produce new states of matter, one may singly produce some of the new R -even states directly via s -channel resonances. In the minimal supersymmetric standard model (MSSM), this means direct production of the heavy scalar and pseudoscalar Higgs bosons, H and A , respectively. Indeed, LHC measurements of the properties of the light Higgs boson h so far have shown it to be nearly standard model (SM)-like [4]. This situation is expected in the decoupling regime, where the heavy SUSY Higgs bosons, and possibly also many sparticles, are well beyond the current LHC reach. (A very SM-like light Higgs boson can also be obtained in the alignment regime [5–7], where the new Higgs bosons, H and A , need not be so heavy.)

The most stringent LHC Run 2 limits on heavy Higgs bosons have been obtained by the ATLAS [8] and CMS [9] collaborations by searching for $H, A \rightarrow \tau\bar{\tau}$ with $\sim 139 \text{ fb}^{-1}$ of integrated luminosity. These heavy Higgs search limits are presented in the m_A vs. $\tan\beta$ plane within the so-called m_h^{125} scenario as proposed by Bagnaschi et al. in ref. [10]. In the m_h^{125} benchmark scenario, most SUSY particles are taken to be at or around the 2 TeV scale, with a SUSY μ parameter at $\mu = 1$ TeV. This ensures that SUSY particles only slightly affect the heavy Higgs searches, and that the dominant H and A decay modes are into SM particles. The ATLAS exclusion contour (which is shown later in this manuscript) shows that the Higgs decoupling limit with a heavy SUSY spectrum is now a likely possibility, particularly since LHC Run 2 limits with $\sim 139 \text{ fb}^{-1}$ of integrated luminosity seem to require

gluino masses $m_{\tilde{g}} \gtrsim 2.2$ TeV [11,12] and top squark masses $m_{\tilde{t}_1} \gtrsim 1.2$ TeV [13–15], at least within the framework of simplified models, which are used for many LHC search results.

In benchmark scenarios, such as the m_h^{125} or the hMSSM [16,17] (in the hMSSM, the light Higgs mass is used as an input to ensure that $m_h = 125$ GeV throughout the heavy Higgs search plane), it is hard to understand why the magnitude of the weak scale $m_{weak} \sim m_{W,Z,h}$ is only ~ 100 GeV whilst sparticles, especially higgsinos, are at the TeV or beyond scale. This brings up the SUSY naturalness question [3] since it may be hard to maintain the MSSM as a plausible theory unless it naturally accommodates the measured value of the weak scale.

In this work, we adopt the measured value of the Z-boson mass as representative of the magnitude of weak scale, where in the MSSM, the Z mass is related to the weak scale Lagrangian parameters via the electroweak minimization condition

$$m_Z^2/2 = \frac{m_{H_d}^2 + \Sigma_d^d - (m_{H_u}^2 + \Sigma_u^u) \tan^2 \beta}{\tan^2 \beta - 1} - \mu^2 \tag{1}$$

where $m_{H_u}^2$ and $m_{H_d}^2$ are the Higgs soft breaking masses, μ is the (SUSY preserving) superpotential μ parameter, and the Σ_d^d and Σ_u^u terms contain a large assortment of loop corrections (see Appendix of ref. [18] and also [19] for leading two-loop corrections). Here, we adopt the notion of practical naturalness [20], wherein an observable \mathcal{O} is natural if all independent contributions to \mathcal{O} are comparable to (Here, the word *comparable* means to within a factor of a few.) or less than \mathcal{O} . For natural SUSY models, we use the naturalness measure [21]:

$$\Delta_{EW} \equiv |\text{maximal term on the right-hand-side of Equation (1)}| / (m_Z^2/2), \tag{2}$$

where a value

$$\Delta_{EW} \lesssim 30 \tag{3}$$

is adopted to fulfill the *comparable* condition of practical naturalness. In many cases, the superpotential μ parameter is taken to be a free parameter and can thus be tuned to cancel against other large contributions to the weak scale arising from SUSY breaking. However, since the μ parameter arises from very different physics than SUSY breaking, e.g., from whatever solution to the SUSY μ problem that is surmised, (=twenty solutions to the SUSY μ problem were recently reviewed in ref. [22]), then such a “just-so” cancellation seems highly implausible (though not impossible) compared to the case where all contributions to the weak scale are of order m_{weak} , in which case μ (or any other parameter) need not be fine-tuned.

Several important implications of Equation (3) arise which are relevant for heavy neutral SUSY Higgs searches:

- The superpotential μ parameter enters Equation (2) directly at tree level, implying that $|\mu| \lesssim 350$ GeV. This means that for heavy Higgs searches with $m_{A,H} \gtrsim 2|\mu|$, then SUSY decay modes of H, A should already be open. If these additional decay widths to SUSY particles are substantial, then the heavy Higgs branching ratios to the usually assumed SM search modes will be significantly reduced.
- For $m_{H_d} \gg m_{H_u}$, then m_{H_d} sets the heavy Higgs mass scale ($m_{A,H} \sim m_{H_d}$) while m_{H_u} sets the mass scale for $m_{W,Z,h}$. Then naturalness requires [23]

$$m_{A,H} \lesssim m_Z \tan \beta \sqrt{\Delta_{EW}}. \tag{4}$$

For $\Delta_{EW} \lesssim 30$ and $\tan \beta \sim 10$, then the value of m_A can range up to ~ 5 TeV. For $\tan \beta$ even higher than ~ 40 , then m_A stays natural all the way up to ~ 20 TeV, although for $\tan \beta \gtrsim 20$, then the bottom squark contributions to Σ_u^u can become large and then provide much stronger upper limits on natSUSY sparticle masses [20]).

Since most heavy Higgs boson searches assume dominant $H, A \rightarrow SM$ decay modes, then such results can overestimate the collider reach for these particles. This is because,

in general, the presence of $H, A \rightarrow SUSY$ decay modes will diminish heavy Higgs boson branching fractions to SM particles via, for example, $H, A \rightarrow \tau\bar{\tau}$ or $b\bar{b}$ decays.

The most lucrative H and A search mode for $m_{H,A} \lesssim 1$ TeV appears to be via the $H, A \rightarrow \tau\bar{\tau}$ mode. This decay mode is enhanced at large $\tan\beta$, and, unlike the $H, A \rightarrow b\bar{b}$ decay mode, does not suffer from large QCD backgrounds. Furthermore, the narrow, low charge multiplicity jets that emerge from τ decay can readily be identified. In refs. [8,9], the ATLAS and CMS collaborations used tau-jet identification along with the cluster transverse mass variable to extract back-to-back (BtB) ditau signal events in their heavy Higgs search results. Results were derived using $\sqrt{s} = 13$ TeV pp collisions with ~ 139 fb $^{-1}$ of integrated luminosity. No signal above the background was seen, so limits were placed in the m_A vs. $\tan\beta$ plane assuming simplified heavy Higgs benchmark scenarios, such as hMSSM [16,17] or the m_h^{125} scenario from ref. [10]. In these scenarios, the SUSY particles are assumed to be too heavy to substantially influence the $H, A \rightarrow \tau\bar{\tau}$ branching fractions. Typical limits from ATLAS [8] are that, for $\tan\beta = 10$, then $m_A \gtrsim 1.1$ TeV while for $\tan\beta = 40$, then $m_A \gtrsim 1.8$ TeV. In addition, in the same (or similar) scenarios, the projected HL-LHC reach for $H, A \rightarrow \tau\bar{\tau}$ was estimated assuming $\sqrt{s} = 14$ TeV and 3000 fb $^{-1}$ of integrated luminosity [24,25]. In these studies, the 95% CL LHC reach for $H, A \rightarrow \tau\bar{\tau}$ for $\tan\beta = 10$ extended out to $m_A \sim 1.35$ TeV and for $\tan\beta = 40$ out to $m_A \sim 2.25$ TeV.

In ref. [26], we previously examined the LHC Run 3 and HL-LHC reach for $H, A \rightarrow \tau\bar{\tau}$ in a natural SUSY benchmark model, dubbed $m_h^{125}(\text{nat})$. In that benchmark, the lightest electroweakinos (EWinos) are higgsino-like, with mass of just a few hundred GeV. The heaviest EWinos are wino-like, with mass ~ 1 TeV. Thus, once $m_{H,A} \gtrsim m(\text{higgsino}) + m(\text{wino})$, then the decay modes $H, A \rightarrow \text{wino} + \text{higgsino}$ (which proceed via the *unsuppressed* gaugino–higgsino–Higgs boson coupling) become dominant unless $\tan\beta$ is very large, at mass values $m_{A,H}$ in the range of LHC search limits. Using the perhaps more plausible $m_h^{125}(\text{nat})$ scenario, the search limits become reduced compared to LHC search results due to the turn-on of the dominant supersymmetric decay modes. In ref. [26], a non-back-to-back ditau signal is also explored, which allows for a ditau invariant mass value $m_{\tau\tau}$ to be computed on an event-by-event basis, with $m_{\tau\tau}$ yielding a (broad) peak around $m_{\tau\tau} \sim m_{H,A}$. The $m_{\tau\tau}$ distribution helps separate the signal from SM backgrounds, especially those arising from $Z \rightarrow \tau\bar{\tau}$. By combining the BtB and non-BtB channels, the discovery/exclusion reach is somewhat enhanced compared to using just the BtB channel.

Taking heed that for $m_{A,H} \gtrsim m(\text{wino}) + m(\text{higgsino})$, heavy Higgs decays to EWino pairs become dominant, in the present paper, we examine prospects for LHC discovery/exclusion by looking at Higgs signals from these supersymmetric decay modes. Decays of heavy SUSY Higgs boson to SUSY particles were originally explored in refs. [27–29], but only in ref. [23] were these decay modes examined in the context of natural SUSY. In that work, it was noted that for $H, A \rightarrow \text{wino} + \text{higgsino}$ channels, the higgsino decays led to mainly soft, quasi-visible decay debris, whilst the winos decayed dominantly via two-body modes into $W + \text{higgsino}$, $Z + \text{higgsino}$ and $h + \text{higgsino}$. The dominant search channels could then be categorized as 1. $h \rightarrow b\bar{b} + E_T$, 2. $Z \rightarrow \ell\bar{\ell} + E_T$ and 3. $W \rightarrow \ell\nu_\ell + E_T$. The last of these seemed plagued by huge backgrounds from SM processes, such as $W + \text{jets}$ and WZ production, while the first two also appeared daunting. In refs. [30,31], some of these same signatures were also examined, although mainly in the context of pMSSM, instead of natural SUSY. For some related works, see also [32–35].

In Section 2 of this paper, we examine production cross sections along with the branching ratios for the dominant decays of the heavy Higgs H and A of the MSSM. Over a wide range of parameters, the SUSY modes dominate the SM decay modes once the kinematic decay thresholds are passed. In Section 3, we identify the main final state channels, which are available for discovery of $H, A \rightarrow SUSY$ in natural SUSY models. In Section 3.1, we examine the $W(\rightarrow \ell\nu) + E_T$ signal channel, and confirm that this is swamped by the SM background, at least at LHC luminosity upgrades. In Section 3.2, we examine the $Z(\rightarrow \ell\bar{\ell}) + E_T$ channel. In Section 3.3, we examine the $h(\rightarrow b\bar{b}) + E_T$ channel and in Section 3.4, we study the signal from h or $Z(\rightarrow \tau\bar{\tau}) + E_T$ events. We identify the

$h(\rightarrow b\bar{b}) + \cancel{E}_T$ channel as the most promising. We also examine whether the signal in these channels can be further enhanced over SM backgrounds by requiring additional soft leptons from the subsequent decays of the higgsinos. In Section 4, we combine signal significance from these various channels (and others containing soft leptons coming from light higgsino decays) to plot the expected HL-LHC discovery and exclusion contours in the m_A vs. $\tan\beta$ plane. Typically, these new $H, A \rightarrow SUSY$ discovery channels may be accessible at HL-LHC for $m_A \sim 1\text{--}2$ TeV (depending somewhat on $\tan\beta$). Our summary and conclusions are contained in Section 5.

2. Production of H and A Followed by Dominant Decay to SUSY Particles

2.1. A Natural SUSY Benchmark Point

For illustrative purposes, we here adopt a similar natural SUSY benchmark point as in ref. [26], which was dubbed $m_h^{125}(\text{nat})$ since the value of m_h is very close to its measured value throughout the entire m_A vs. $\tan\beta$ plane. We use the two-extra-parameter non-universal Higgs model (NUHM2) [36] with parameter space

$$m_0, m_{1/2}, A_0, \tan\beta, \mu, m_A \quad (5)$$

where the first three parameters are GUT scale entries, whilst the latter three parameters are weak scale entries. This form of NUHM2 input parameters is convenient for naturalness studies of the SUSY Higgs sector since μ can be set to its natural range of $\mu \sim 100\text{--}350$ GeV, whilst both m_A and $\tan\beta$ are free parameters. (The NUHM2 framework allows for independent soft SUSY breaking mass parameters for the scalar fields H_u and H_d in the Higgs sector, but leaves the matter scalar mass parameters universal to avoid flavor problems. The high-scale parameters $m_{\tilde{H}_u}^2$ and $m_{\tilde{H}_d}^2$ are then traded for weak-scale parameters μ and m_A in Equation (6).) We adopt the following natural SUSY benchmark Higgs search scenario:

$$m_h^{125}(\text{nat}) : m_0 = 5 \text{ TeV}, m_{1/2} = 1 \text{ TeV}, A_0 = -1.6m_0, \tan\beta, \mu = 200 \text{ GeV and } m_A. \quad (6)$$

(A similar $m_h^{125}(\text{nat})$ benchmark model spectrum, but with $\mu = 250$ GeV and $m_{1/2} = 1.2$ TeV, is shown in Table 1 of ref. [26] for $\tan\beta = 10$ and $m_A = 2$ TeV.) For our $m_h^{125}(\text{nat})$ scenario, large negative values of the trilinear soft term A_0 are expected since these reduce the values of $\Sigma_u^H(\tilde{t}_{1,2})$ in Equation (1) via cancellations in their expressions [21]. For natural SUSY models emergent from the string landscape, A_0 is statistically selected to large values, but not so large as to result in charge-or-color-breaking (CCB) minima of the scalar potential: see, for example, Figure 1 of ref. [37].

We adopt the computer code Isajet [38] for spectrum generation and computation of dark matter observables and other low energy observables for comparison with data. (We note that the value of $\sigma^{SI}(\tilde{\chi}_1^0, p)$ from Table 1 appears to be in conflict with the recent bounds from the LZ experiment [39] by about a factor of 3 (see also results from Xenon1T [40] and PandaX-II [41]) on the direct detection of WIMP scattering on their liquid Xe target, even taking into account that the relic neutralinos are thermally underproduced with the remainder of dark matter composed of, for example, axions [42], or something else. We are not particularly concerned by this since it is easy to imagine that entropy dilution from late decaying saxions or moduli [43] fields could further reduce the neutralino relic abundance, bringing the BM point into accord with limits from direct detection [44] with no impact upon the LHC phenomenology discussed in this paper. A similar situation is obtained for the benchmark case considered here.) The benchmark (BM) point spectrum and some associated observables are shown in Table 1. The SUSY Higgs boson masses are computed using the renormalization-group (RG) improved third-generation fermion/sfermion loop corrections [45]. The RG-improved Yukawa couplings include full threshold corrections [46], which account for leading two-loop effects [47] in the Higgs mass calculation. For $\tan\beta = 10$ and $m_A = 2$ TeV, we note that $\Delta_{EW} = 15$ so the model is indeed EW natural. Additionally, with $m_h = 124.5$ GeV, $m_{\tilde{g}} = 2.4$ TeV and $m_{\tilde{t}_1} = 1.6$ TeV, it is consistent with the LHC Run 2 SUSY search constraints. Most relevant to this paper, the two lightest neutralinos, $\tilde{\chi}_1^0$

and $\tilde{\chi}_2^0$, and the lighter chargino, $\tilde{\chi}_1^\pm$, are higgsino-like with masses ~ 200 GeV, while the neutralino $\tilde{\chi}_3^0$ is bino-like with a mass of 450 GeV and the heaviest neutralino and the heavier chargino have masses ~ 0.86 TeV. Thus, the $H, A \rightarrow \text{wino} + \text{higgsino}$ decay modes turn on for $m_{H,A} \gtrsim 1.1$ TeV (although $H, A \rightarrow \text{bino} + \text{higgsino}$ turns on at somewhat lower m_A values).

Table 1. Input parameters (TeV) and masses (GeV) for the $m_h^{125}(\text{nat})$ SUSY benchmark point from the NUHM2 model with $m_t = 173.2$ GeV using Isajet 7.88 [38].

Parameter	$m_h^{125}(\text{nat})$
m_0	5 TeV
$m_{1/2}$	1 TeV
A_0	−8 TeV
$\tan \beta$	10
μ	200 GeV
m_A	2 TeV
$m_{\tilde{g}}$	2423 GeV
$m_{\tilde{u}_L}$	5294 GeV
$m_{\tilde{u}_R}$	5433 GeV
$m_{\tilde{e}_R}$	4813 GeV
$m_{\tilde{t}_1}$	1584 GeV
$m_{\tilde{t}_2}$	3770 GeV
$m_{\tilde{b}_1}$	3801 GeV
$m_{\tilde{b}_2}$	5158 GeV
$m_{\tilde{\tau}_1}$	4739 GeV
$m_{\tilde{\tau}_2}$	5094 GeV
$m_{\tilde{\nu}_\tau}$	5191 GeV
$m_{\tilde{\chi}_1^\pm}$	208.6 GeV
$m_{\tilde{\chi}_2^\pm}$	855.9 GeV
$m_{\tilde{\chi}_1^0}$	195.5 GeV
$m_{\tilde{\chi}_2^0}$	208.6 GeV
$m_{\tilde{\chi}_3^0}$	451.6 GeV
$m_{\tilde{\chi}_4^0}$	868.0 GeV
m_h	124.5 GeV
$\Omega_{\tilde{z}_1}^{std} h^2$	0.011
$BF(b \rightarrow s\gamma) \times 10^4$	3.1
$BF(B_s \rightarrow \mu^+ \mu^-) \times 10^9$	3.8
$\sigma^{SI}(\tilde{\chi}_1^0, p)$ (pb)	3.0×10^{-9}
$\sigma^{SD}(\tilde{\chi}_1^0, p)$ (pb)	6.1×10^{-5}
$\langle \sigma v \rangle _{v \rightarrow 0}$ (cm ³ /sec)	2.0×10^{-25}
Δ_{EW}	15

Some (Cosmological) Aspects of Our Benchmark (BM) Point

The low value of $\mu \sim 200$ GeV for our $m_h^{125}(\text{nat})$ scenario BM point leads to a higgsino-like LSP and thermally underproduced dark matter over the entire range of naturalness allowed μ values: $\mu \sim 100\text{--}350$ GeV. We also require a natural solution to the strong CP problem, which then requires the presence of an axion (and concomitant axino and saxion component fields) in the low-energy effective theory. (We restrict discussion to the SUSY DFSZ model [48,49], where the required two-Higgs doublets neatly mesh into the MSSM framework, which also requires two Higgs doublets.) The required global Peccei–Quinn (PQ) symmetry may be generated as an approximate accidental symmetry (since global symmetries are incompatible with quantum gravity) arising from some more fundamental discrete symmetry (such as discrete R -symmetries [50]), which might arise from string compactifications [51]. Such models have been written down in, for example, refs. [52,53]. In these models, the PQ breaking needed for the axion is generated due to SUSY breaking, thus linking the PQ scale f_a to the hidden sector SUSY breaking scale such

that $f_a \sim 10^{11}$ GeV in the cosmological sweet spot. In such a case, dark matter consists of mainly axions [54] with a subdominant component of higgsino-like WIMPs, which may escape direct and indirect detection bounds due to their depleted abundance [42]. In this type of (well-motivated) dark matter scenario, there is no fine-tuning required to obtain the measured abundance of dark matter.

In such a gravity-mediated context, we expect the presence of a gravitino with mass $m_{3/2} \sim m_0 \sim$ of tens of TeV [55]. Such gravitinos may be thermally produced in the early universe and disrupt standard Big Bang nucleosynthesis (BBN) bounds due to their late decays, provided the re-heat temperature after inflation $T_R \gtrsim 10^9$ GeV [56]. While this scenario creates tension with standard leptogenesis (which requires $T_R \gtrsim 2 \times 10^9$ GeV) [57], other baryogenesis scenarios, such as non-thermal leptogenesis or Dine–Randall–Thomas leptogenesis [58], are still operative at much lower values of T_R [59].

2.2. H and A Production Cross Sections at LHC

In Figure 1, we show the total cross sections for (a) $pp \rightarrow H + X$ and (b) $pp \rightarrow A + X$ production in the m_A vs. $\tan \beta$ plane using the computer code SusHi [60], which includes leading NNLO corrections. The plots show σ in fb units for $\sqrt{s} = 14$ TeV. The dominant production processes come from the gg and $b\bar{b}$ fusion diagrams, with the latter dominating unless $\tan \beta$ is very small. In the figure, the total production cross section is color coded with cross sections ranging as high as $\sigma \sim 10^5$ fb on the left edge, although this region is now LHC-excluded. For the LHC-allowed regions, where, for example, $m_A \gtrsim 1$ TeV for $\tan \beta \sim 10$, then the cross sections lie typically below 10 fb. Of course, the σ values drop off for increasing m_A but also we see how they increase for increasing $\tan \beta$. For any given value of m_A and $\tan \beta$, the production cross sections for $pp \rightarrow H$ and $pp \rightarrow A$ are typically very close in value to each other.

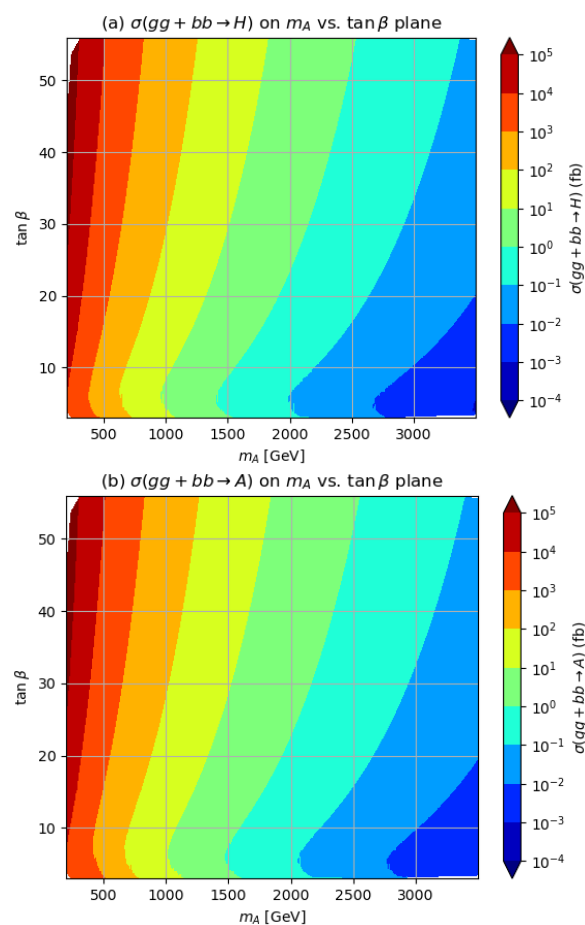


Figure 1. The total cross section for (a) $pp \rightarrow H$ and (b) $pp \rightarrow A$ at $\sqrt{s} = 14$ TeV using the SusHi code [60].

2.3. H and A Branching Fractions

In Figures 2 and 3, we show some select H and A branching fractions (BFs) in the m_A vs. $\tan\beta$ plane. The branching fractions are again color coded, with the larger ones denoted by red whilst the smallest ones are denoted by dark blue. The branching fractions are extracted from the Isasugra code [38], and the decay formulae can be found in Appendix C of ref. [1].

In Figure 2a, we show the BF for $H \rightarrow b\bar{b}$. This decay mode to SM particles is indeed dominant for $m_A \lesssim 1$ TeV and for larger values of $\tan\beta \gtrsim 10$ –20. In Figure 2b, we show the BF($H \rightarrow \tau\bar{\tau}$). Like $H \rightarrow b\bar{b}$, this mode is enhanced at large $\tan\beta$ and has provided the best avenue for heavy Higgs discovery/exclusion plots so far.

While SUSY decay modes of H and A to higgsino pairs are also open in these regions, these decay modes are suppressed by mixing angles. In the MSSM, there is a direct gauge coupling [1]

$$\mathcal{L} \ni -\sqrt{2} \sum_{i,A} S_i^\dagger g t_A \bar{\lambda}_A \psi_i + H.c. \quad (7)$$

where S_i labels various matter and Higgs scalar fields, ψ_i is the fermionic superpartner of S_i and λ_A is the gaugino with gauge index A . Additionally, g is the corresponding gauge coupling for the gauge group in question, and the t_A are the corresponding gauge group matrices. For the case where S_i is the Higgs scalar fields, then there is an unsuppressed coupling of the Higgs scalars into gaugino plus higgsino (as mentioned earlier). This coupling can then lead to dominant heavy SUSY Higgs boson decays to SUSY particles when the gaugino+higgsino decay channel is kinematically open and unsuppressed. However, it also shows why the heavy Higgs decay to higgsino pairs is suppressed by mixing angles for $|\mu| \ll |M_{1,2}|$, once we recognize that a Higgs boson–higgsino–higgsino coupling is forbidden by gauge invariance.

In Figure 2c, we show BF($H \rightarrow \tilde{\chi}_1^\pm \tilde{\chi}_2^\mp$), where $\tilde{\chi}_1^\pm$ is dominantly higgsino-like and $\tilde{\chi}_2^\pm$ is dominantly wino-like for natural SUSY models, such as the m_h^{125} (nat) scenario. Here, we see that for larger values of $m_A \simeq m_H \gtrsim 1.2$ TeV, then this mode turns on, and at least for moderate $\tan\beta \sim 10$ –20 (which is favored by naturalness [23]), rapidly comes to dominate the H decay modes along with the neutral wino+higgsino channels $H \rightarrow \tilde{\chi}_1^0 \tilde{\chi}_4^0$ (Figure 2d) and $H \rightarrow \tilde{\chi}_2^0 \tilde{\chi}_4^0$ (Figure 2e). Here, $\tilde{\chi}_4^0$ is mainly neutral wino-like while $\tilde{\chi}_{1,2}^0$ are mainly higgsino-like. The sum of these three wino+higgsino decay channels thus dominates the H decay branching fractions for $m_{H,A} \gtrsim 1.2$ TeV and low-to-moderate values of $\tan\beta$. For high values of $\tan\beta$, the bottom and τ Yukawa couplings become large, and SM decays to fermions once again dominate SUSY decays. Decays of H to gauge boson pairs are unimportant in the decoupling limit. For completeness, we also show in Figure 2f) the decay mode $H \rightarrow \tilde{\chi}_1^0 \tilde{\chi}_3^0$ which is to higgsino+bino. This mode is large only in a small region of $m_H \sim 1$ TeV and modest $\tan\beta$, where the mode $H \rightarrow \text{bino} + \text{higgsino}$ decay is turned on, but where $H \rightarrow \text{wino} + \text{higgsino}$ has yet to become kinematically open. Decays to winos dominate decays to binos because the $SU(2)$ gauge coupling is larger than the hypercharge gauge coupling.

In Figure 3, we show the same branching fractions as in Figure 2, but this time for A decay. The plots are very similar to the results from Figure 2, and for largely the same reasons. For $m_A \gtrsim 1.2$ TeV and small-to-moderate $\tan\beta$, then $A \rightarrow \text{wino} + \text{higgsino}$ becomes the dominant A decay mode. We note that A does not couple to vector boson pairs.

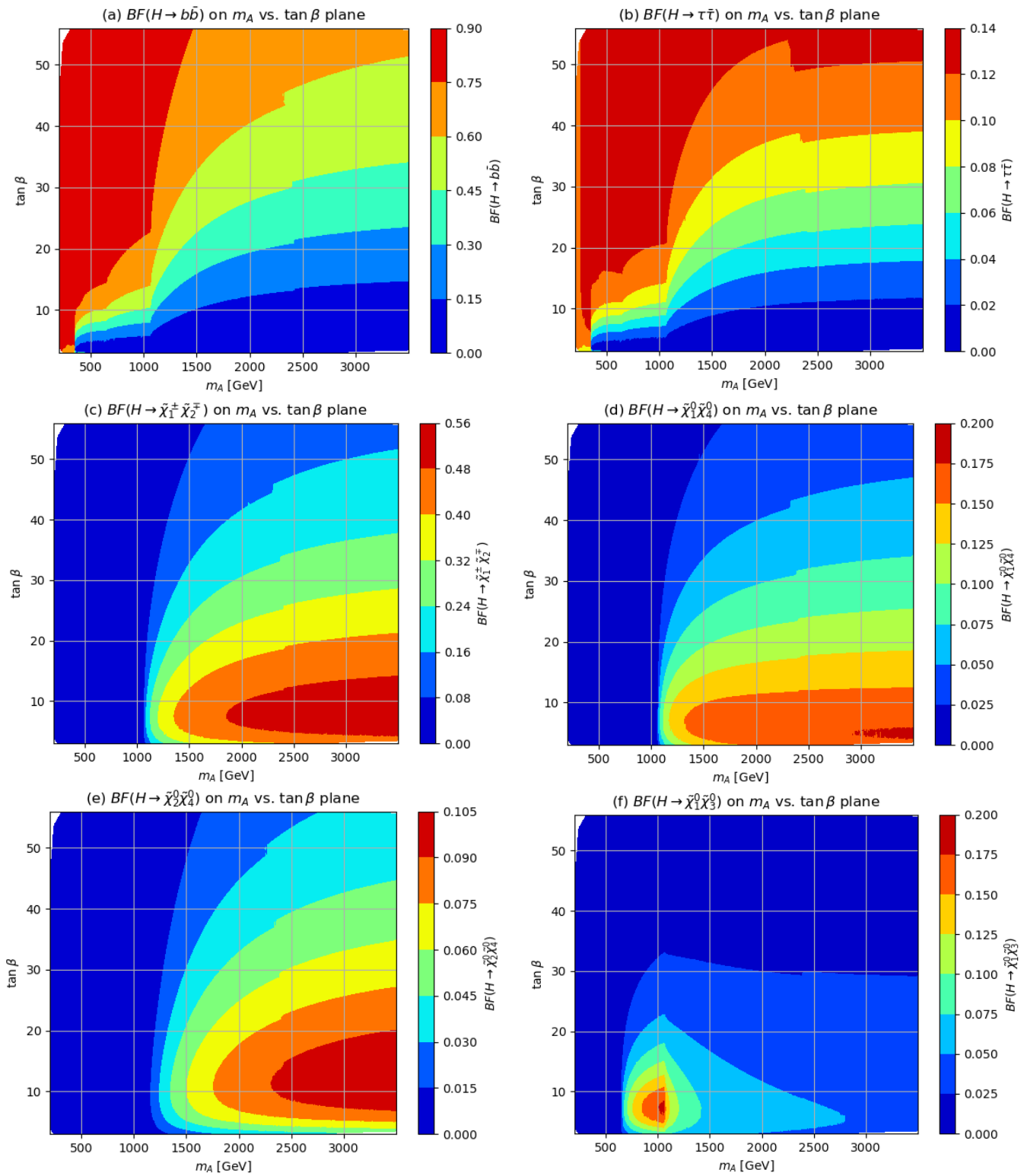


Figure 2. Branching fractions for H to (a) $b\bar{b}$, (b) $\tau\bar{\tau}$, (c) $\tilde{\chi}_1^\pm \tilde{\chi}_2^\mp$, (d) $\tilde{\chi}_1^0 \tilde{\chi}_4^0$, (e) $\tilde{\chi}_2^0 \tilde{\chi}_4^0$ and (f) $\tilde{\chi}_1^0 \tilde{\chi}_3^0$ from Isajet 7.88 [38].

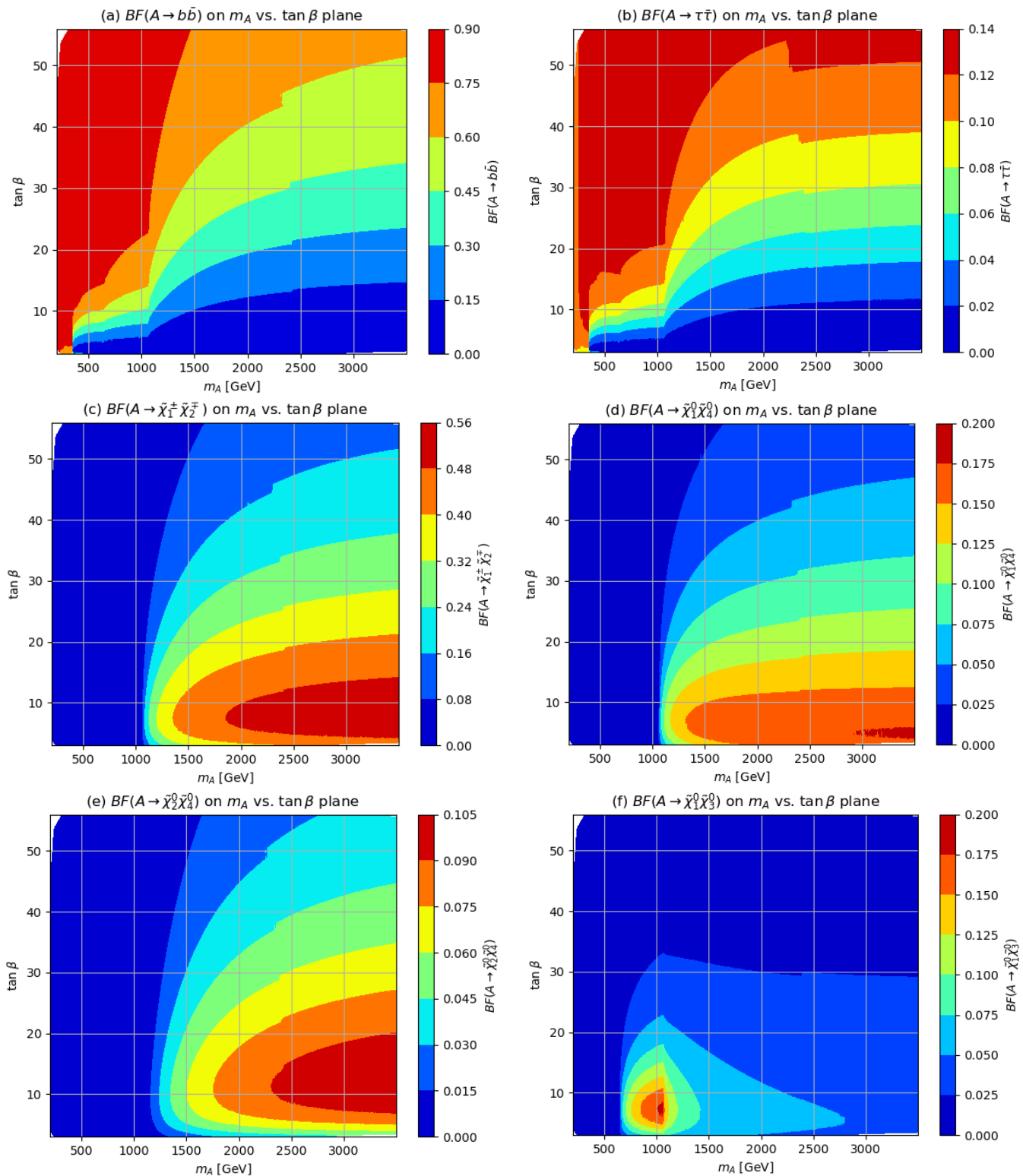


Figure 3. Branching fractions for A to (a) $b\bar{b}$, (b) $\tau\bar{\tau}$, (c) $\tilde{\chi}_1^\pm\tilde{\chi}_2^\mp$, (d) $\tilde{\chi}_1^0\tilde{\chi}_4^0$, (e) $\tilde{\chi}_2^0\tilde{\chi}_4^0$ and (f) $\tilde{\chi}_1^0\tilde{\chi}_3^0$ from Isajet 7.88 [38].

3. A Survey of Various $H, A \rightarrow SUSY$ Signal Channels

Having established that the SUSY decay modes of H and A may dominate soon after they become kinematically allowed, we explore the ensuing $H, A \rightarrow SUSY$ signatures for LHC upgrades in order to determine if they can open new avenues to discovery or, perhaps, confirmation of a signal seen via a SM channel. The dominant H and A decay modes are to

neutral and charged winos plus light higgsinos, where the light higgsinos, if they are not LSP, decay to very soft visible SM particles. The $\tilde{\chi}_4^0$, which in our case is mainly neutral wino, typically decays via $\tilde{\chi}_4^0 \rightarrow W^\pm \tilde{\chi}_1^\mp$ with a branching fraction $\sim 50\%$, while the decays $\tilde{\chi}_4^0 \rightarrow Z \tilde{\chi}_{1,2}^0$ and to $\tilde{\chi}_4^0 \rightarrow h \tilde{\chi}_{1,2}^0$ each have branching fractions $\sim 25\%$. The $\tilde{\chi}_2^\pm$, which is mainly charged wino, decays via $\tilde{\chi}_2^- \rightarrow W^- \tilde{\chi}_{1,2}^0 \sim 50\%$ of the time, with $\tilde{\chi}_2^- \rightarrow Z \tilde{\chi}_1^-$ and $h \tilde{\chi}_1^-$ each have branching fractions $\sim 25\%$. Combining the decay patterns, the dominant $H, A \rightarrow SUSY$ decay modes lead to the following signatures:

- $H, A \rightarrow W + E_T$,
- $H, A \rightarrow Z + E_T$ and
- $H, A \rightarrow h + E_T$.

Each of these signatures may also contain some soft leptons or jets which arise from the light higgsino decays; these soft visibles potentially can lead to further discovery channels, or at least enhance the discovery/exclusion channels if the SM backgrounds are under control.

For our simulations, we generate signal SUSY Les Houches Accord (SLHA) output files using Isajet [38] and feed these into Pythia [61] for event generation. We then interface Pythia with the Delphes [62] toy detector simulation code. The SM backgrounds of $pp \rightarrow W, \gamma^*/Z, t\bar{t}, VV$ ($V = W$ or Z), Wh and Zh production are all generated using Pythia.

For all events, we require that they pass one of our baseline trigger requirements:

- Baseline small-radius jet (SRj): Using anti- k_T jet finder algorithm, require $p_T(SRj) > 25$ GeV with jet cone size $\Delta R < 0.4$ and $|\eta_{SRj}| < 4.5$.
- Baseline large-radius jet (LRj): Using anti- k_T jet finder algorithm, require $p_T(LRj) > 100$ GeV with jet cone size $\Delta R < 1.2$ and $|\eta_{LRj}| < 4.5$, for all signatures except for $1LRj + \ell + E_T$, for which $\Delta R < 1.5$. The large-radius jets are formed using calorimeter deposits (or track information for muons) so that even isolated leptons (see below) are included as constituents of these jets. This will be especially important for the signal examined in Section 3.4 below.
- Baseline isolated lepton: Satisfy basic Delphes lepton isolation requirement with $p_T(\ell) > 5$ GeV, lepton cone size $\Delta R < 0.3$, and $pTRatio(e) < 0.1$ while $pTRatio(\mu) < 0.2$, where $pTRatio$ is defined in Delphes as $\frac{\sum_i |p_{Ti}|}{p_T(\ell)}$, for calorimetric cells within the lepton cone.

For the signal search, we further require the following:

- SRj: Satisfy above SRj requirement plus $|\eta_{SRj}| < 2.4$.
- b -jets: Satisfy above SRj requirement plus b -jet tagged by Delphes b -tagging requirement.
- Signal leptons: Require above-baseline lepton qualities plus $p_T(e) > 20$ GeV with $|\eta(e)| < 2.47$, while $p_T(\mu) > 25$ GeV with $|\eta(\mu)| < 2.5$.

We examined several distributions for four cases with $m_A = 1.5$ and 2 TeV, and $\tan \beta = 10$ and 40 to arrive at suitable cuts for the various signals from $H, A \rightarrow \text{gaugino} + \text{higgsino}$ decays that we discuss in the remainder of this section.

3.1. $H, A \rightarrow W(\rightarrow \ell\nu) + E_T$ Signal

For the $H, A \rightarrow W + E_T$ channel, we will look for $W \rightarrow \ell\nu_\ell$ where $\ell = e$ or μ . We first require the following:

- Exactly one baseline lepton (and no LRjs, which will comprise an alternative channel: see below). This lepton should also satisfy signal lepton requirements.

After examining various distributions, we require the following:

- $|\eta(\ell)| < 1.3$;
- $E_T > 150$ GeV;
- $\Delta\phi(\ell, E_T) > 90^\circ$;
- Transverse mass $m_T(\ell, E_T) > 100$ GeV;
- $p_T(W) > 20$ GeV where $\vec{p}_T(W) = \vec{p}_T(\ell) + \vec{E}_T$.

Our goal in each signal channel is to look for an excess above the SM backgrounds in the largest transverse mass bins, which are most sensitive to the TeV-scale heavy Higgs decay. Our basic results are shown in Figure 4, where we plot two signal benchmark cases: one for $m_A = 1.5$ with $\tan \beta = 40$ (black-dashed) and one for $m_A = 2$ TeV with $\tan \beta = 10$ (orange-dashed). The SM BG distributions are color coded as solid (unstacked) histograms. (We are aware that the $m_A = 1.5$ TeV, $\tan \beta = 40$ BM case is just excluded at 95%CL by the ATLAS search for heavy Higgs bosons, assuming that H, A decays essentially only via SM modes [8].) As anticipated [23], there is an enormous SM BG from direct off-shell W production, as indicated by the pink histogram. The next largest SM BGs come from $t\bar{t}$, WW and WZ production (yellow, red and green histograms). Over the entire range of m_T , the SM BGs lie several orders of magnitude above our SUSY BM models. Thus, it appears to be extremely difficult to root out a signal via the single lepton channel.

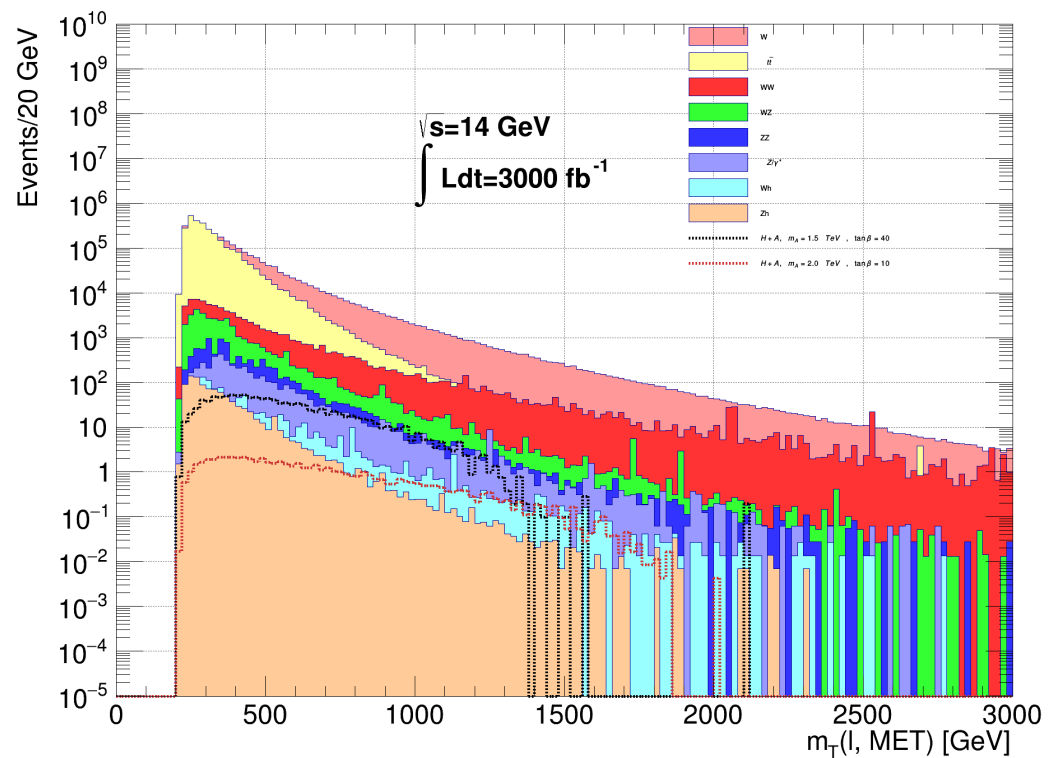


Figure 4. Distribution in $m_T(\ell, E_T)$ for $pp \rightarrow H, A \rightarrow W + E_T$ events. We show two signal distributions (dashed) along with dominant SM backgrounds (not stacked).

3.2. $H, A \rightarrow Z(\rightarrow \ell\bar{\ell}) + E_T$ Signal

In this channel, we search for a high momentum, leptonically decaying Z boson recoiling against E_T . Here, we require the following:

- Exactly two baseline leptons (veto additional leptons).
- The two leptons satisfy signal lepton requirements and are opposite-sign/same flavor (OS/SF).
- The dilepton pair invariant mass reconstructs m_Z : $80 \text{ GeV} < m(\ell\bar{\ell}) < 100 \text{ GeV}$.

We also require the following:

- $E_T > 250 \text{ GeV}$;
- $E_{T,rel} := E_T \cdot \sin(\min(\Delta\phi, \frac{\pi}{2})) > 125 \text{ GeV}$; where $\Delta\phi$ is the azimuthal angle between the \vec{E}_T and the closest lepton or jet with $p_T > 25 \text{ GeV}$;
- $|\eta(\ell_1)| < 1.3$, $|\eta(\ell_2)| < 2$ ($p_T(\ell_1) > p_T(\ell_2)$) and $|\eta(\ell\bar{\ell})| < 1.5$;
- $\Delta\phi(\ell\bar{\ell}, E_T) > 140^\circ$;
- $\Delta\phi(\ell_1, \ell_2) < 80^\circ$;
- $|\vec{p}_T(Z) + \vec{E}_T| > 25 \text{ GeV}$.

We then plot the cluster transverse mass [63] $m_{cT}(\ell\bar{\ell}, \cancel{E}_T)$ in Figure 5. From the figure, we see that the dominant SM backgrounds come from the ZZ and WZ production followed by subdominant Zh production. For the signal from our benchmark point with $m_A = 1.5$ TeV and $\tan\beta = 40$ (black-dashed histogram), we see that signal exceeds WZ background around $m_{cT} \sim 1200$ GeV and is only a factor of ~ 2 below the dominant ZZ BG. Thus, we might expect a significant shape deviation in the $m_{cT}(\ell\bar{\ell}, \cancel{E}_T)$ distribution at large transverse mass values, signaling the presence of a heavy, new physics object contributing to this distribution.

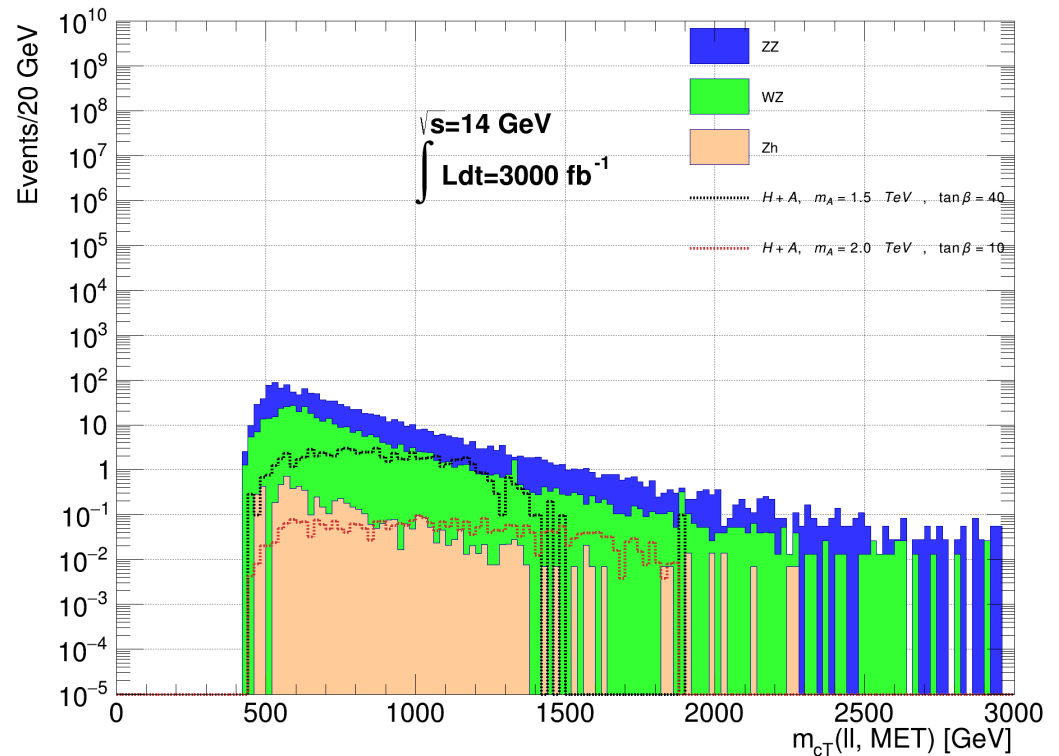


Figure 5. Distribution in $m_{cT}(\ell\bar{\ell}, \cancel{E}_T)$ for $pp \rightarrow H, A \rightarrow Z + \cancel{E}_T$ with $Z \rightarrow \ell^+ \ell^-$ decay events at $\sqrt{s} = 14$ TeV. We show two signal distributions (dashed) along with dominant SM backgrounds (not stacked).

3.3. $H, A \rightarrow h(\rightarrow b\bar{b}) + \cancel{E}_T$ Signal

In this case, we search for the production of a single SM-like Higgs boson recoiling against large \cancel{E}_T , with $h \rightarrow b\bar{b}$. Here, we require the following:

- At least two tagged b -jets;
- Veto any baseline leptons;
- Exactly one LRj;
- At least two b -jets within the cone of the LRj;
- Exactly one di- b -jet pair within the cone of the LRj reconstructs the light Higgs mass: $90 \text{ GeV} < m(bb) < 135 \text{ GeV}$;
- $m(LRj) - m(bb) > -5 \text{ GeV}$.

We further require the following:

- $\cancel{E}_T > 225 \text{ GeV}$;
- $\cancel{E}_{T,rel} > 225 \text{ GeV}$;
- $H_T > 350 \text{ GeV}$;
- $p_T(b_1) > 100 \text{ GeV}$;
- $p_T(bb) / p_T(LRj) > 0.9$;
- $m(bb) / p_T(LRj) > 0.9$;
- $|\eta(bb)| < 1.4$;

- $\Delta\phi(bb, E_T) > 145^\circ$;
- $\max[\Delta\phi(j, LRj)] < 140^\circ$ where j loops over all baseline SR jets in the event;
- $\Delta\phi(b_1, b_2) < 65^\circ$.

Here, H_T is the scalar sum of E_T s of all visible objects in the event. We plot the ensuing $m_{cT}(b\bar{b}, E_T)$ distribution in Figure 6. From the figure, we see that the dominant SM backgrounds come from $t\bar{t}$ production (where the b -jets accidentally reconstruct the Higgs boson mass) followed by Zh and then ZZ production. In this case, at large $m_{cT} \gtrsim 1$ TeV, the $\tan\beta = 40$, $m_A = 1.5$ TeV BM case is actually comparable to SM backgrounds. Thus, we would expect a measurable shape deviation in this distribution at high values of cluster transverse mass, for at least some of our BM points.

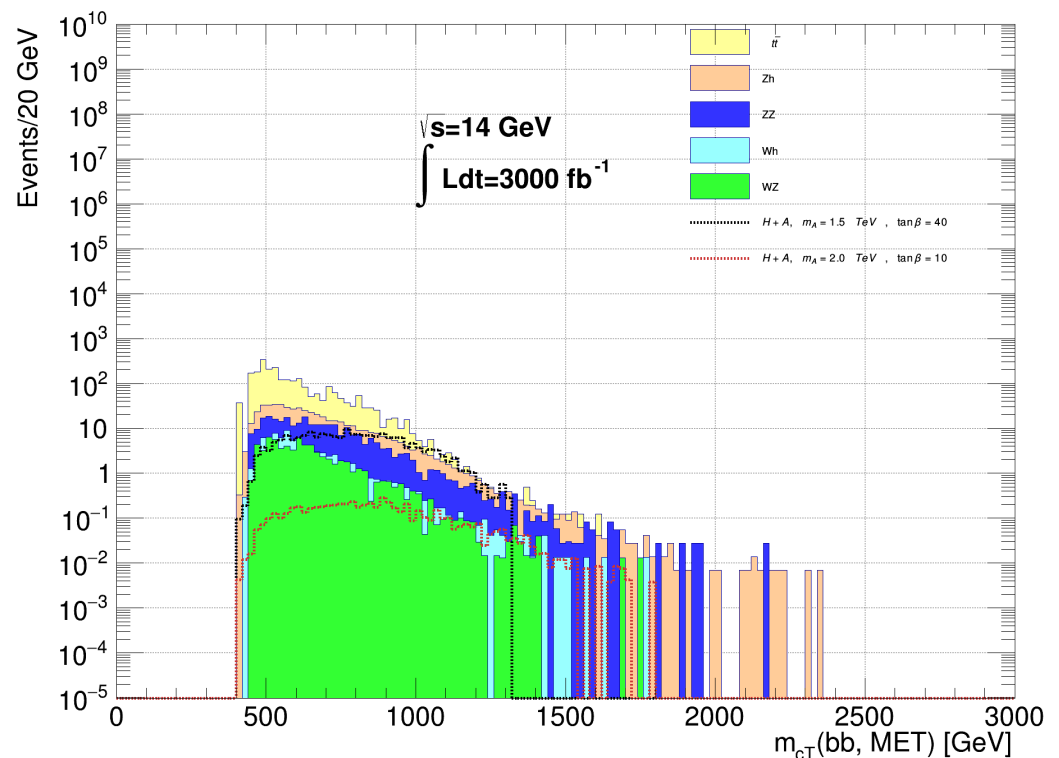


Figure 6. Distribution in $m_{cT}(b\bar{b}, E_T)$ for $pp \rightarrow H, A \rightarrow h + E_T$ with $h \rightarrow b\bar{b}$ decay events at $\sqrt{s} = 14$ TeV. We show two signal distributions (dashed) along with dominant SM backgrounds (not stacked).

3.4. $H, A \rightarrow 1LRj + \ell + E_T$ Signal

Here, we examine the prospects for observing the signal from H, A decays that yield a high p_T Z or h boson plus E_T , where the Z or the h decays into tau pairs, and one of the taus decays hadronically and the other leptonically. Such a topology will yield an SRj plus an isolated signal lepton that coalesces to a single LRj that includes an identified lepton within a cone with $\Delta R < 1.5$.

For this channel, we require the following:

- Exactly one signal lepton and no additional baseline leptons in the event.
- Exactly one LRj with invariant mass $40 \text{ GeV} < m(LRj) < 145 \text{ GeV}$ in accord with a source of either W, Z (or h).
- The lepton is within the cone of the LRj.

In addition, we require the following:

- $E_T > 275 \text{ GeV}$;
- $E_{T,rel} > 125 \text{ GeV}$;
- $|\eta(\ell)| < 1.7$;
- $H_T > 350 \text{ GeV}$;

- $\Delta\phi(LRj, E_T) > 140^\circ$;
- $p_T(\ell) / p_T(LRj) > 0.9$;
- No b -jet within cone of the LRj;
- No jets with $p_T(j) > 100$ GeV outside the cone of the LRj.

We next plot the resulting $m_{cT}(LRj, \cancel{E}_T)$ distribution (not including the lepton) in Figure 7. From the plot, we see that the largest BGs come from WW , WZ and ZZ production. While BG exceeds signal at low m_{cT} , the largest signal distributions are close to the BGs around $m_{cT} \sim 1000$ GeV. Thus, this channel might offer a confirming signal to a bulge in the large transverse mass distribution from one of the above cases.

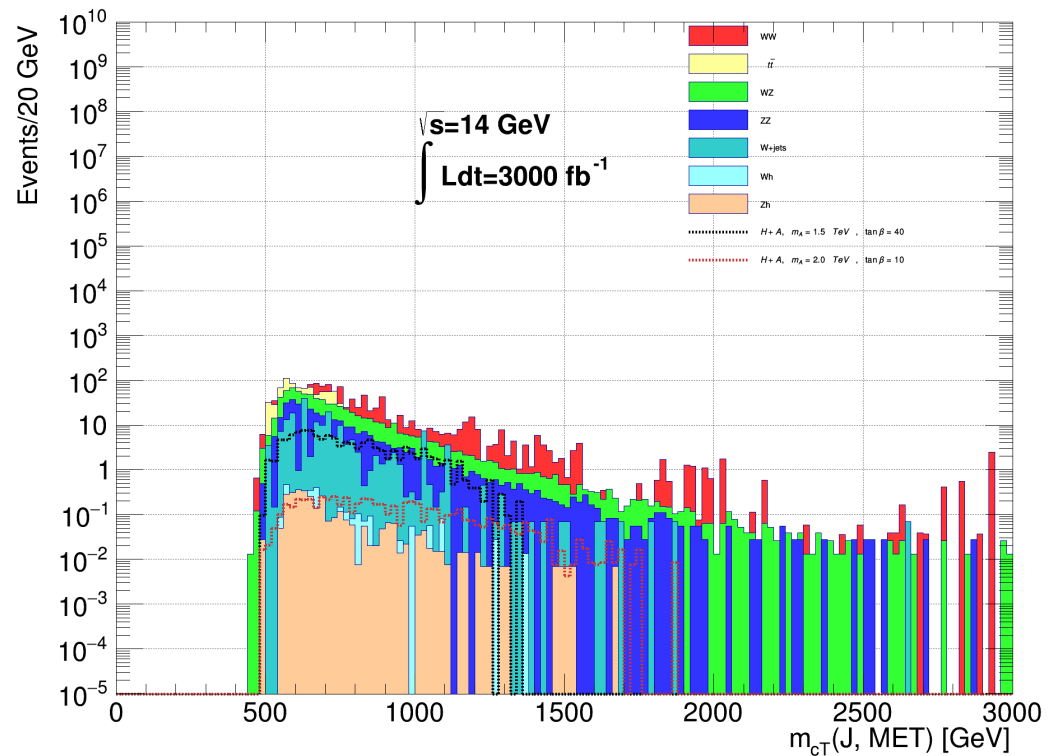


Figure 7. Distribution in $m_{cT}(LRj, \cancel{E}_T)$ for $pp \rightarrow H, A \rightarrow LRj + \ell + \cancel{E}_T$ events at $\sqrt{s} = 14$ TeV. We show two signal distributions (dashed) along with dominant SM backgrounds (not stacked).

In the next two subsections, we attempt to see whether the signals in the high p_T $h(\rightarrow b\bar{b}) + E_T$ and high p_T $Z(\rightarrow \ell\bar{\ell}) + E_T$ channels can be further enhanced by requiring additional soft leptons from the decays of the higgsinos. However, before turning to this discussion, we mention that we had also attempted to examine the study the signal from hadronically decaying high p_T Z and W bosons $+ E_T$ events (without any additional soft leptons) but found that it was hopelessly overwhelmed by the background $Z \rightarrow \nu\bar{\nu} + \text{jet}$ production.

3.5. $H, A \rightarrow 3\ell + E_T$ Signal

Here, we attempt to pick out $Z \rightarrow \ell\bar{\ell} + E_T$ events that occur along with a soft lepton from light higgsino decay. Thus, we require the following:

- Exactly three baseline leptons.
- At least two leptons satisfy the signal lepton requirement.
- At least two leptons are OS/SF leptons.
- At least one OS/SF pair satisfies the Z -mass requirement: $80 \text{ GeV} < m(\ell\bar{\ell}) < 100 \text{ GeV}$; if more than one pair satisfy the Z -mass, then the pair closest to m_Z is chosen whilst the third is designated ℓ_3 .

In addition, we require the following:

- $E_T \geq 200$ GeV;
- $E_{T,rel} > 25$ GeV;
- $p_T(\ell_3) < 30$ GeV;
- $|\eta(\ell_s)| < 1.5$; $|\eta(\ell\bar{\ell})| < 1.3$;
- $\Delta\phi(\ell\bar{\ell}, E_T) > 125^\circ$;
- $\Delta\phi(\ell_1\ell_2) < 55^\circ$;
- $|\vec{p}_T(Z) + \vec{p}_T(\ell_3 E_T)| > 20$ GeV.

The resultant cluster transverse mass distribution $m_{cT}(3\ell, E_T)$ is shown in Figure 8. We see that, as might be expected, the largest SM BG comes from WZ production. At very large $m_{cT}(3\ell, E_T) \gtrsim 1.2$ TeV, our largest signal BM point is comparable to SM BG levels. However, in the best case, only a small number of signal events will populate this region. Thus, this channel may offer, at best, some corroborative evidence for a $H, A \rightarrow SUSY$ signal.

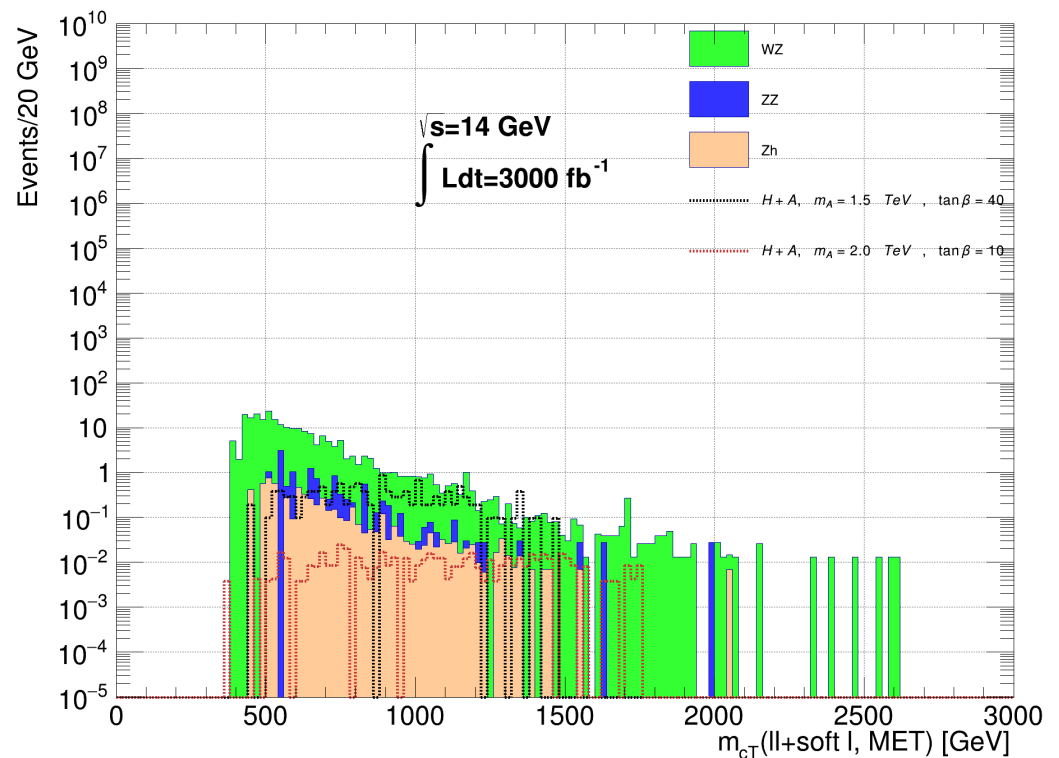


Figure 8. Distribution in $m_{cT}(3\ell, E_T)$ for $pp \rightarrow H, A \rightarrow 3\ell + E_T$ events at $\sqrt{s} = 14$ TeV. We show two signal distributions (dashed) along with dominant SM backgrounds (not stacked).

3.6. $H, A(\rightarrow bb) + \ell + E_T$ Signal

Finally, we attempt to capture an $h \rightarrow b\bar{b} + E_T$ signal, where there is an additional soft lepton from light higgsino decay. For this, we require the following:

- At least two b -jet candidates;
- At least one baseline lepton;
- Exactly one LRj;
- At least two b -jets within the cone of the LRj;
- Exactly one pair of b -jets within the cone of the LRj reconstructs the light Higgs:
 $90 \text{ GeV} < m(bb) < 135 \text{ GeV}$;
- $m(LRj) - m(bb) > -5 \text{ GeV}$, and
- $m(bb)/p_T(LRj) > 0.9$.

Then, we also require the following:

- $E_T > 225$ GeV;
- $E_{T,rel} > 200$ GeV;
- $p_T(\ell) < 30$ GeV for any ℓ in the event;
- $p_T(b_1) > 100$ GeV;
- $p_T(bb) / p_T(LRj) > 0.9$;
- $|\eta(bb)| < 2$;
- $\Delta\phi(bb, E_T) > 145^\circ$;
- $\max[\Delta\phi(j, LRj)] < 150^\circ$, where j cycles over all SR jets in the event, and
- $\Delta\phi(b_1, b_2) < 65^\circ$.

The cluster transverse mass distribution $m_{cT}(bb\ell, E_T)$ distribution is shown in Figure 9. The largest BG comes from $t\bar{t}$ production, where again the two b -jets accidentally have $m_{bb} \sim m_H$, with smaller contributions from Wh and WZ production. At very large m_{cT} values, a signal may emerge from BG although the high energy tail is very much rate limited.

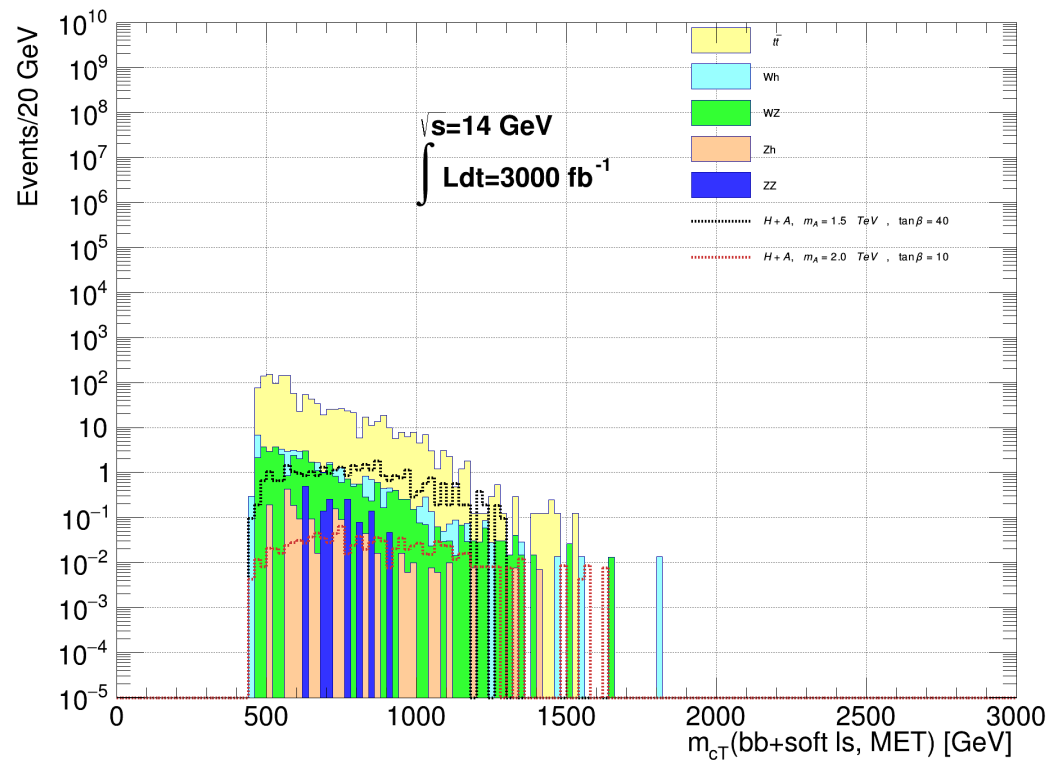


Figure 9. Distribution in $m_{cT}(bb\ell, E_T)$ for $pp \rightarrow H, A \rightarrow bb\ell + E_T$ events at $\sqrt{s} = 14$ TeV. We show two signal distributions (dashed) along with dominant SM backgrounds (not stacked).

4. Regions of the m_A vs. $\tan \beta$ Plane Accessible to HL-LHC

After adopting the above cuts for the various signal channels, we can now create reach plots in terms of discovery sensitivity or exclusion limits for $pp \rightarrow H, A \rightarrow SUSY$ in the m_A vs. $\tan \beta$ plane. We use the 5σ level to denote the heavy Higgs discovery and assume the true distribution one observes experimentally corresponds to signal-plus-background. We then test this against the background-only distribution in order to see if the background-only hypothesis can be rejected at the 5σ level. Specifically, we use the binned transverse mass distributions (bin width of 20 GeV) from each signal channel as displayed above to obtain the discovery/exclusion limits.

In the case of the exclusion plane, the upper limits for exclusion of a signal are set at 95% CL; one assumes that the true distribution that one observes in experiment corresponds to background-only. The limits are then computed using a modified frequentist CL_s method [64], where the profile likelihood ratio is the test statistic. In both the exclusion and

discovery planes, the asymptotic approximation for obtaining the median significance is employed [65]. The systematic uncertainty is then assumed to be 1σ of the corresponding statistical uncertainty: a very conservative rule-of-thumb estimate.

In Figure 10, we plot our main results for the discovery/exclusion regions for HL-LHC with $\sqrt{s} = 14$ TeV and 3000 fb^{-1} of integrated luminosity in the m_A vs. $\tan\beta$ plane using our $m_h^{125}(\text{nat})$ benchmark scenario (which is quite typical for natural SUSY models [3]). In Figure 10a, we plot the 5σ discovery reach using the strongest channel, which is the $H, A \rightarrow h + E_T$ with $h \rightarrow b\bar{b}$. The solid black line denotes the computed reach, while the green and yellow bands display the $\pm 1\sigma$ and $\pm 2\sigma$ uncertainty. From the plot, we see that a discovery region does indeed exist, starting around $m_A \sim 1$ TeV where $H, A \rightarrow \text{gaugino} + \text{higgsino}$ begins to turn on. For this channel, the discovery region extends out to $m_A \sim 1.5$ TeV for high $\tan\beta$ where the increasing H, A production cross section compensates for the decreasing $H, A \rightarrow \text{SUSY}$ branching fractions. The discovery region pinches off below $\tan\beta \sim 10$, where the $pp \rightarrow H, A$ production rates become too small, mainly because the bottom quark Yukawa coupling becomes small. In Figure 10b, we plot the 95% CL exclusion limit for HL-LHC in the $b\bar{b} + E_T$ channel. While this plot has the same low m_A kinematic cutoff, the exclusion limit now extends out to $m_A \sim 1.85$ TeV for large $\tan\beta \sim 40\text{--}50$. We also see that the exclusion contour extends well below $\tan\beta \sim 10$. The region above the blue dashed contour in the frames in the right-hand column is excluded at the 95%CL by the ATLAS search with an integrated luminosity of 139 fb^{-1} [8] for the signal from $H, A \rightarrow \tau\bar{\tau}$ decays, albeit in the m_h^{125} scenario, where the H and A essentially decay only via SM modes. If SUSY decay decays of H and A are important, these will reduce the branching fractions for the decays to tau pairs, and the allowed region to the right of the blue contour will be somewhat larger.

In Figure 10c, we plot the 5σ discovery contour, but this time, we combine the two strongest channels: $b\bar{b} + E_T$ and $\ell^+ \ell^- + E_T$. The added channel from $H, A \rightarrow Z + E_T$ has a similar lower cutoff (as expected) around $m_A \sim 1$ TeV but now extends to $m_A \sim 1.65$ TeV for high $\tan\beta$ —an increase in discovery reach by ~ 150 GeV from the Figure 10a result. The corresponding 95% CL exclusion from the two combined channels is shown in Figure 10d, where the high $\tan\beta$ limit now extends out to $m_A \sim 2$ TeV, again a gain in the m_A reach of ~ 150 GeV.

In Figure 10e, we show the HL-LHC 5σ discovery reach contour, which is gained by combining all six signal channels from Section 3. In this case, the discovery reach starts at the same kinematic cutoff, but now extends as high as $m_A \sim 1.75$ TeV, a gain in the reach of 250 GeV over the single-channel results from Figure 10a. In Figure 10f, we plot the corresponding 95% CL exclusion contour from the combined six signal channels. For this case, the contour now extends to $m_A \sim 2.15$ TeV at high $\tan\beta$; this is a gain in the m_A reach of ~ 300 GeV over the single channel exclusion results from Figure 10b. Meanwhile, the exclusion contour extends well below $\tan\beta \sim 10$ in the lower portion of the plot.

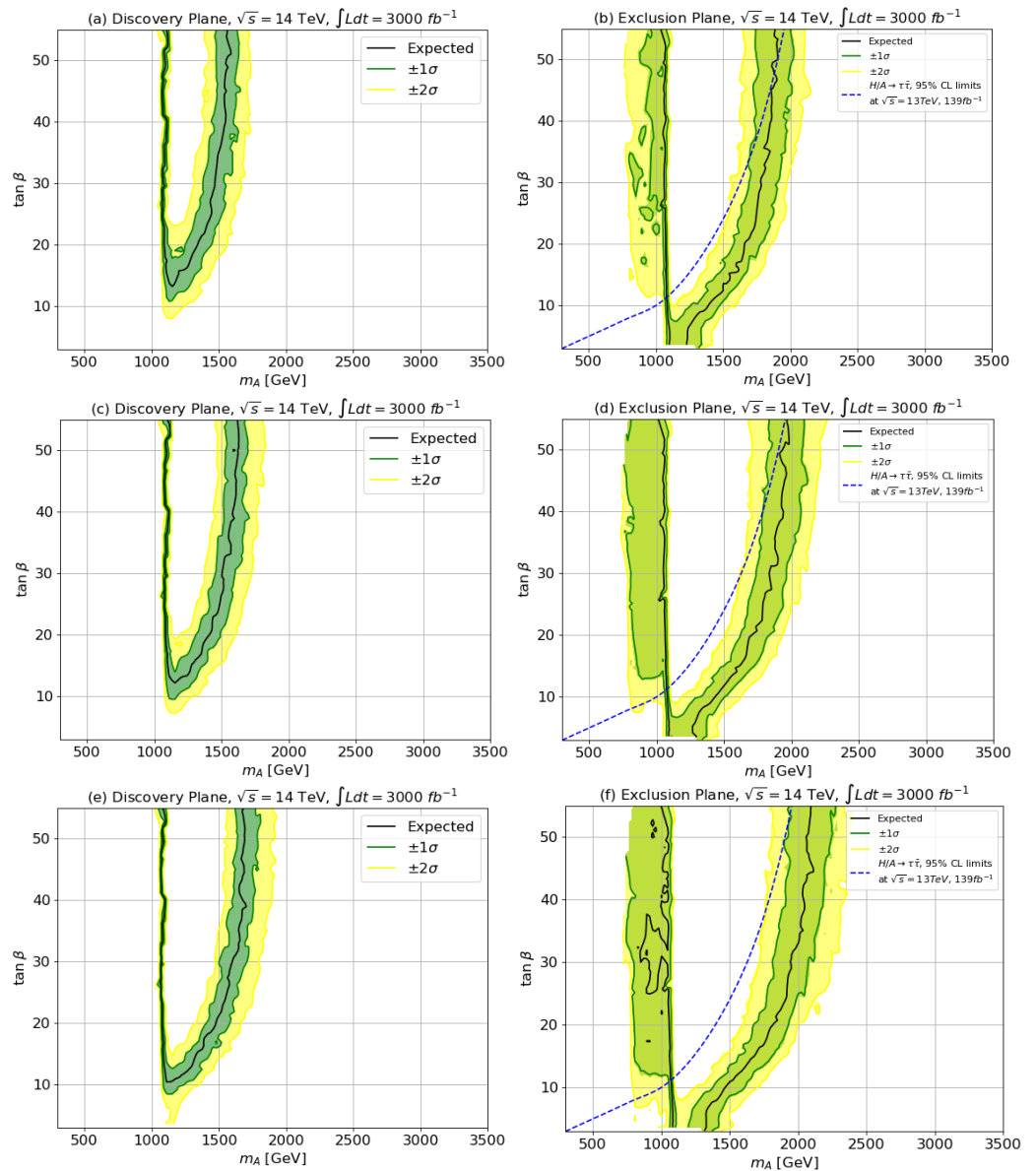


Figure 10. In frame (a), we plot the HL-LHC 5σ discovery contours for $H, A \rightarrow b\bar{b} + E_T$ events with $\sqrt{s} = 14$ TeV and 3000 fb^{-1} . In frame (b), we plot the corresponding 95% CL exclusion limit. In frame (c), we plot the 5σ discovery reach via the combined $b\bar{b} + E_T$ and $\ell\bar{\ell} + E_T$ channels. In (d), we plot the corresponding 95% CL exclusion. In (e), we show the 5σ contour combining all six discovery channels, while in (f) we plot the 95% CL exclusion limits from all six channels combined. The region above the dashed contour in the frames in the right-hand column is excluded at the 95%CL by ATLAS, although in the m_h^{125} scenario, the H and A essentially decay only via SM modes.

To illustrate how the significance increases with the increasing number of signal channels which are included, we list in Table 2 our calculated significances for our $\tan\beta = 40$, $m_A = 1.5$ TeV BM point, assuming 3000 fb^{-1} of integrated luminosity. Our main purpose here is to illustrate the relative contributions of each SUSY channel to the significance. For this BM case with just the $b\bar{b} + E_T$ channel, we already have a significance of 5.53. As we include more signal channels, the significance climbs to over 7σ for this particularly favorable BM point.

Table 2. Significance of the signal for six different signal channels for our BM point with $\tan \beta = 40$ and $m_A = 1.5$ TeV at HL-LHC with 3000 fb^{-1} .

Signal Channel	Significance
$b\bar{b}$	5.53
$b\bar{b} + 2\ell$	6.25
$b\bar{b} + 2\ell + \ell LRj$	6.92
$b\bar{b} + 2\ell + \ell LRj + \ell 2b$	7.14
$b\bar{b} + 2\ell + \ell LRj + \ell 2b + 3\ell$	7.47
$b\bar{b} + 2\ell + \ell LRj + \ell 2b + 3\ell + 1\ell$	7.54

Before closing, we note that non-resonant wino–higgsino associated production from $q\bar{q}$ collisions in the $m_h^{125}(\text{nat})$ scenario will be suppressed because squarks are heavy and wino–higgsino mixing is small. We explicitly checked that for the BM point considered here, the contribution from the continuum is well below the resonance contribution, even for the $\tan \beta = 10$ case shown in Figures 4–7. Thus, an observation of any signal in these channels will be indicative not only of SUSY, but also of the production of heavy Higgs bosons. We also remark that, at the LHC, gaugino–higgsino-associated production may be kinematically accessible, even when the gaugino pair production channel might be kinematically suppressed, while higgsino pair production events (without an additional radiated hard jet or photon) are buried under SM backgrounds.

5. Conclusions

In this paper, we studied the prospects of HL-LHC to detect the heavy neutral Higgs bosons of natural SUSY models via their decays into SUSY particles. Natural SUSY models may be regarded as the most plausible of SUSY scenarios since they naturally explain why the weak scale lies in the $m_{W,Z,h} \sim 100$ GeV range, whilst the SUSY breaking scale is in the (multi-)TeV range. It was argued that SUSY models with radiatively driven naturalness [18,21] are expected to be the most likely to emerge from string landscape statistics; the landscape then actually predicts $m_h \sim 125$ GeV with sparticles beyond the present LHC search limits [3].

For this class of models, with light higgsinos and TeV-scale gauginos, heavy neutral Higgs bosons decay dominantly to *gaugino + higgsino* once these modes are kinematically allowed, provided $\tan \beta$ is not very large. The SUSY decay modes diminish the usually assumed SM decay modes (such as $H, A \rightarrow \tau\bar{\tau}$) while opening new discovery possibilities. Here, we identify the most promising discovery channels as $W + E_T, Z + E_T$ and $h + E_T$, where the W, Z or h come from the decay of the heavy gaugino daughter. We proposed sets of cuts designed to optimize the extraction of signals from background. While $W + E_T$ is beset with huge SM backgrounds, mainly from direct W production, the $h(\rightarrow b\bar{b}) + E_T, Z(\rightarrow \ell\bar{\ell}) + E_T$ and $(Z \text{ or } h) \rightarrow \tau\bar{\tau} + E_T$ channels are much more promising. We also examined the possibility that the signal would be enhanced by requiring additional (soft) leptons from the decay of the higgsinos.

Specifically, in each of these channels, we analyzed various binned transverse mass distributions for signal plus background to test against the background-only hypothesis to obtain 5σ discovery contours and 95% CL exclusion contours in the m_A vs. $\tan \beta$ plane at the HL LHC. Our main result is shown in Figure 10, where we show the reach plots for the following: (1) the strongest channel, $h + E_T$ where $h \rightarrow b\bar{b}$, (2) this channel combined with the next strongest $Z(\rightarrow \ell\bar{\ell})$ channel, and 3) for all six $H, A \rightarrow \text{SUSY}$ discovery channels. The $H, A \rightarrow \text{SUSY}$ signal can occur at viable levels for $m_A \sim 1\text{--}2.1$ TeV for large $\tan \beta \gtrsim 30$ with lower exclusion contours for lower $\tan \beta$, where H, A production rates become much smaller. We can compare our reach for $H, A \rightarrow \text{SUSY}$ discovery channels to the recently computed discovery reach via the $H, A \rightarrow \tau\bar{\tau}$ mode as presented in ref. [26]. In that work, it was found that even with SUSY decay modes allowed in the same $m_h^{125}(\text{nat})$ scenario, the discovery/exclusion contours extend well past the $H, A \rightarrow \text{SUSY}$ modes, which were investigated here. This is perhaps due to the advantages of $m(\tau\bar{\tau})$ reconstructing

a resonance around $m(\tau\bar{\tau}) \sim m_A$ and in general lower SM background levels for the $\tau\bar{\tau}$ channel. It would be very instructive to examine the impact of the SUSY decays of the heavy Higgs bosons on future hadron colliders, such as FCChh, where the larger center-of-mass energy would allow for the production of Higgs bosons with masses of several TeV and kinematically unsuppressed decays to SUSY particles.

Author Contributions: Conceptualization, H.B., V.B., X.T. and K.Z.; methodology, K.Z.; software, K.Z.; validation, H.B., V.B., X.T. and K.Z.; formal analysis, H.B., V.B., X.T. and K.Z.; investigation, H.B. and K.Z.; resources, V.B.; data curation, n/a; writing-original draft preparation, H.B.; writing-review and editing, H.B., V.B., X.T. and K.Z.; visualization, n/a; supervision, H.B., V.B., X.T. and K.Z.; project administration, H.B., V.B., X.T. and K.Z.; funding acquisition, H.B. and V.B. All authors have read and agreed to the published version of the manuscript.

Funding: This research was funded by the U.S. Department of Energy, Office of Science, Office of High Energy Physics under Award Number DE-SC-0009956 and DE-SC-0017647.

Data Availability Statement: Not applicable.

Acknowledgments: This material is based upon work supported by the U.S. Department of Energy, Office of Science, Office of High Energy Physics under Award Number DE-SC-0009956 and DE-SC-0017647.

Conflicts of Interest: The authors declare no conflict of interest.

References

1. Baer, H.; Tata, X. *Weak Scale Supersymmetry: From Superfields to Scattering Events*; Cambridge University Press: Cambridge, UK, 2006.
2. Drees, M.; Godbole, R.; Roy, P. *Theory and Phenomenology of Sparticles: An Account of Four-Dimensional $N = 1$ Supersymmetry in High Energy Physics*; World Scientific: Singapore, 2004.
3. Baer, H.; Barger, V.; Salam, S.; Sengupta, D.; Sinha, K. Status of weak scale supersymmetry after LHC Run 2 and ton-scale noble liquid WIMP searches. *Eur. Phys. J. Spec. Top.* **2020**, *229*, 3085–3141.
4. Cadamuro, L. Higgs boson couplings and properties. *PoS LHCP* **2019**, *2019*, 101. [[CrossRef](#)]
5. Gunion, J.F.; Haber, H.E. The CP conserving two Higgs doublet model: The Approach to the decoupling limit. *Phys. Rev. D* **2003**, *67*, 075019. [[CrossRef](#)]
6. Craig, N.; Galloway, J.; Thomas, S. Searching for Signs of the Second Higgs Doublet. *arXiv* **2013**, arXiv:1305.2424.
7. Carena, M.; Low, I.; Shah, N.R.; Wagner, C.E.M. Impersonating the Standard Model Higgs Boson: Alignment without Decoupling. *JHEP* **2014**, *4*, 15.
8. Aad, G.; Abbott, B.; Abbott, D.C.; Abbott, A.; Abed Abud, K.; Abeling, D.K.; Abhayasinghe, S.H.; Abidi, O.S.; AbouZeid, N.L.; Abraham, H.; et al. Search for heavy Higgs bosons decaying into two tau leptons with the ATLAS detector using pp collisions at $\sqrt{s} = 13$ TeV. *Phys. Rev. Lett.* **2020**, *125*, 051801. [[CrossRef](#)]
9. CMS Collaboration. Searches for additional Higgs bosons and for vector leptoquarks in $\tau\tau$ final states in proton-proton collisions at $\sqrt{s} = 13$ TeV. *arXiv* **2022**, arXiv:2208.02717.
10. Bagnaschi, E.; Bahl, H.; Fuchs, E.; Hahn, T.; Heinemeyer, S.; Liebler, S.; Patel, S.; Slavich, P.; Stefaniak, T.; Wagner, C.E.M.; et al. MSSM Higgs Boson Searches at the LHC: Benchmark Scenarios for Run 2 and Beyond. *Eur. Phys. J. C* **2019**, *79*, 617.
11. ATLAS Collaboration. Search for squarks and gluinos in final states with jets and missing transverse momentum using 139 fb⁻¹ of $\sqrt{s} = 13$ TeV pp collision data with the ATLAS detector. *JHEP* **2021**, *2*, 143.
12. Sirunyan, A.M.; Tumasyan, A.; Adam, W.; Ambrogio, F.; Bergauer, T.; Brandstetter, J.; Dragicevic, M.; Erö, J.; Valle, A.E.D.; Flechl, M.; et al. Search for supersymmetry in proton-proton collisions at 13 TeV in final states with jets and missing transverse momentum. *JHEP* **2019**, *10*, 244.
13. ATLAS Collaboration. Search for a scalar partner of the top quark in the all-hadronic $t\bar{t}$ plus missing transverse momentum final state at $\sqrt{s} = 13$ TeV with the ATLAS detector. *Eur. Phys. J. C* **2020**, *80*, 737.
14. ATLAS Collaboration. Search for new phenomena with top quark pairs in final states with one lepton, jets, and missing transverse momentum in pp collisions at $\sqrt{s} = 13$ TeV with the ATLAS detector. *JHEP* **2021**, *4*, 174.
15. Sirunyan, A.M.; Tumasyan, A.; Adam, W.; Andrejkovic, J.W.; Bergauer, T.; Chatterjee, S.; Dragicevic, M.; Del Valle, A.E.; Fruehwirth, R.; Jeitler, M.; et al. Search for top squark production in fully-hadronic final states in proton-proton collisions at $\sqrt{s} = 13$ TeV. *Phys. Rev. D* **2021**, *104*, 052001. [[CrossRef](#)]
16. Djouadi, A.; Maiani, L.; Moreau, G.; Polosa, A.; Quevillon, J.; Riquer, V. The post-Higgs MSSM scenario: Habemus MSSM? *Eur. Phys. J. C* **2013**, *73*, 2650.
17. Djouadi, A.; Maiani, L.; Polosa, A.; Quevillon, J.; Riquer, V. Fully covering the MSSM Higgs sector at the LHC. *JHEP* **2015**, *6*, 168.

18. Baer, H.; Barger, V.; Huang, P.; Mickelson, D.; Mustafayev, A.; Tata, X. Radiative natural supersymmetry: Reconciling electroweak fine-tuning and the Higgs boson mass. *Phys. Rev. D* **2013**, *87*, 115028.
19. Dedes, A.; Slavich, P. Two loop corrections to radiative electroweak symmetry breaking in the MSSM. *Nucl. Phys. B* **2003**, *657*, 333–354. [[CrossRef](#)]
20. Baer, H.; Barger, V.; Savoy, M. Upper bounds on sparticle masses from naturalness or how to disprove weak scale supersymmetry. *Phys. Rev. D* **2016**, *93*, 035016.
21. Baer, H.; Barger, V.; Huang, P.; Mustafayev, A.; Tata, X. Radiative natural SUSY with a 125 GeV Higgs boson. *Phys. Rev. Lett.* **2012**, *109*, 161802.
22. Bae, K.J.; Baer, H.; Barger, V.; Sengupta, D. Revisiting the SUSY μ problem and its solutions in the LHC era. *Phys. Rev. D* **2019**, *99*, 115027.
23. Bae, K.J.; Baer, H.; Barger, V.; Mickelson, D.; Savoy, M. Implications of naturalness for the heavy Higgs bosons of supersymmetry. *Phys. Rev. D* **2014**, *90*, 075010.
24. Cepeda, M.; Gori, S.; Ilten, P.; Kado, M.; Riva, F.; Khalek, R.A.; Aboubrahim, A.; Alimena, J.; Alioli, S.; Alves, A.; et al. Report from Working Group 2: Higgs Physics at the HL-LHC and HE-LHC. *CERN Yellow Rep. Monogr.* **2019**, *7*, 221–584.
25. Bahl, H.; Bechtler, P.; Heinemeyer, S.; Liebler, S.; Stefaniak, T.; Weiglein, G. HL-LHC and ILC sensitivities in the hunt for heavy Higgs bosons. *Eur. Phys. J. C* **2020**, *80*, 916.
26. Baer, H.; Barger, V.; Tata, X.; Zhang, K. Prospects for Heavy Neutral SUSY HIGGS Scalars in the hMSSM and Natural SUSY at LHC Upgrades. *Symmetry* **2022**, *14*, 2061.
27. Baer, H.; Dicus, D.; Drees, M.; Tata, X. Higgs Boson Signals in Superstring Inspired Models at Hadron Supercolliders. *Phys. Rev. D* **1987**, *36*, 1363. [[CrossRef](#)] [[PubMed](#)]
28. Gunion, J.F.; Haber, H.E.; Drees, M.; Karatas, D.; Tata, X.; Godbole, R. Decays of Higgs Bosons to Neutralinos and Charginos in the Minimal Supersymmetric Model: Calculation and Phenomenology. *Int. J. Mod. Phys. A* **1987**, *2*, 1035. [[CrossRef](#)]
29. Gunion, J.F.; Haber, H.E. Higgs Bosons in Supersymmetric Models. 3. Decays Into Neutralinos and Charginos. *Nucl. Phys. B* **1988**, *307*, 445; Erratum in *Nucl. Phys. B* **1993**, *402*, 569. [[CrossRef](#)]
30. Barman, R.K.; Bhattacharjee, B.; Chakraborty, A.; Choudhury, A. Study of MSSM heavy Higgs bosons decaying into charginos and neutralinos. *Phys. Rev. D* **2016**, *94*, 075013.
31. Adhikary, A.; Bhattacharjee, B.; Godbole, R.M.; Khan, N.; Kulkarni, S. Searching for heavy Higgs in supersymmetric final states at the LHC. *JHEP* **2021**, *4*, 284.
32. Arbey, A.; Battaglia, M.; Mahmoudi, F. Supersymmetric Heavy Higgs Bosons at the LHC. *Phys. Rev. D* **2013**, *88*, 015007.
33. Kulkarni, S.; Lechner, L. Characterizing simplified models for heavy Higgs decays to supersymmetric particles. *arXiv* **2017**, arXiv:1711.00056.
34. Gori, S.; Liu, Z.; Shakya, B. Heavy Higgs as a Portal to the Supersymmetric Electroweak Sector. *JHEP* **2019**, *4*, 049.
35. Bahl, H.; Lozano, V.M.; Weiglein, G. Simplified models for resonant neutral scalar production with missing transverse energy final states. *JHEP* **2022**, *11*, 42.
36. Baer, H.; Mustafayev, A.; Profumo, S.; Belyaev, A.; Tata, X. Direct, indirect and collider detection of neutralino dark matter in SUSY models with non-universal Higgs masses. *JHEP* **2005**, *7*, 65. [[CrossRef](#)]
37. Baer, H.; Barger, V.; Savoy, M.; Serce, H. The Higgs mass and natural supersymmetric spectrum from the landscape. *Phys. Lett. B* **2016**, *758*, 113–117.
38. Paige, F.E.; Protopopescu, S.D.; Baer, H.; Tata, X. ISAJET 7.69: A Monte Carlo event generator for pp, anti-p p, and e+e- reactions. *arXiv* **2003**, arXiv:hep-ph/0312045.
39. Aalbers, J.; Akerib, D.S.; Akerlof, C.W.; Al Musalhi, A.K.; Alder, F.; Alqahtani, A.; Alsum, S.K.; Amarasinghe, C.S.; Ames, A.; Anderson, T.J.; et al. First Dark Matter Search Results from the LUX-ZEPLIN (LZ) Experiment. *arXiv* **2022**, arXiv:2207.03764.
40. XENON Collaboration; Aprile, E.; Aalbers, J.; Agostini, F.; Alfonsi, M.; Althueser, L.; Amaro, F.D.; Anthony, M.; Arneodo, F.; Baudis, L.; et al. Dark Matter Search Results from a One Ton-Year Exposure of XENON1T. *Phys. Rev. Lett.* **2018**, *121*, 111302.
41. Cui, X.; Abdukerim, A.; Chen, W.; Chen, X.; Chen, Y.; Dong, B.; Fang, D.; Fu, C.; Giboni, K.; Giuliani, F.; et al. Dark Matter Results From 54-Ton-Day Exposure of PandaX-II Experiment. *Phys. Rev. Lett.* **2017**, *119*, 181302. [[CrossRef](#)]
42. Baer, H.; Barger, V.; Serce, H. SUSY under siege from direct and indirect WIMP detection experiments. *Phys. Rev. D* **2016**, *94*, 115019.
43. Bae, K.J.; Baer, H.; Barger, V.; Deal, R.W. The cosmological moduli problem and naturalness. *JHEP* **2022**, *2*, 138.
44. Gelmini, G.B.; Gondolo, P. Neutralino with the right cold dark matter abundance in (almost) any supersymmetric model. *Phys. Rev. D* **2006**, *74*, 023510. [[CrossRef](#)]
45. Bisset, M.A. Detection of Higgs Bosons of the Minimal Supersymmetric Standard Model at Hadron Supercolliders. Ph.D. Thesis, University of Hawaii, Honolulu, HI, USA, 1995.
46. Pierce, D.M.; Bagger, J.A.; Matchev, K.T.; Zhang, R.-j. Precision corrections in the minimal supersymmetric standard model. *Nucl. Phys. B* **1997**, *491*, 3–67. [[CrossRef](#)]
47. Carena, M.; Haber, H.E. Higgs Boson Theory and Phenomenology. *Prog. Part. Nucl. Phys.* **2003**, *50*, 63–152. [[CrossRef](#)]
48. Bae, K.J.; Baer, H.; Chun, E.J. Mixed axion/neutralino dark matter in the SUSY DFSZ axion model. *JCAP* **2013**, *12*, 028.
49. Bae, K.J.; Baer, H.; Lessa, A.; Serce, H. Coupled Boltzmann computation of mixed axion neutralino dark matter in the SUSY DFSZ axion model. *JCAP* **2014**, *10*, 82.

50. Lee, H.M.; Raby, S.; Ratz, M.; Ross, G.G.; Schieren, R.; Schmidt-Hoberg, K. Discrete R symmetries for the MSSM and its singlet extensions. *Nucl. Phys. B* **2011**, *850*, 1–30.
51. Nilles, H.P. Stringy Origin of Discrete R-symmetries. *PoS CORFU* **2017**, *2016*, 17.
52. Baer, H.; Barger, V.; Sengupta, D. Gravity safe, electroweak natural axionic solution to strong CP and SUSY μ problems. *Phys. Lett. B* **2019**, *790*, 58–63.
53. Bhattiprolu, P.N.; Martin, S.P. High-quality axions in solutions to the μ problem. *Phys. Rev. D* **2021**, *104*, 055014.
54. Bae, K.J.; Baer, H.; Chun, E.J. Mainly axion cold dark matter from natural supersymmetry. *Phys. Rev. D* **2014**, *89*, 031701.
55. Soni, S.K.; Weldon, H.A. Analysis of the Supersymmetry Breaking Induced by $N = 1$ Supergravity Theories. *Phys. Lett. B* **1983**, *126*, 215–219. [[CrossRef](#)]
56. Kohri, K.; Moroi, T.; Yotsuyanagi, A. Big-bang nucleosynthesis with unstable gravitino and upper bound on the reheating temperature. *Phys. Rev. D* **2006**, *73*, 123511. [[CrossRef](#)]
57. Bardeen, W.A.; Peccei, R.D.; Yanagida, T. CONSTRAINTS ON VARIANT AXION MODELS. *Nucl. Phys. B* **1987**, *279*, 401–428. [[CrossRef](#)]
58. Dine, M.; Randall, L.; Thomas, S.D. Baryogenesis from flat directions of the supersymmetric standard model. *Nucl. Phys. B* **1996**, *458*, 291–326. [[CrossRef](#)]
59. Bae, K.J.; Baer, H.; Serce, H.; Zhang, Y.-F. Leptogenesis scenarios for natural SUSY with mixed axion-higgsino dark matter. *JCAP* **2016**, *1*, 12.
60. Harlander, R.V.; Liebler, S.; Mantler, H. SusHi: A program for the calculation of Higgs production in gluon fusion and bottom-quark annihilation in the Standard Model and the MSSM. *Comput. Phys. Commun.* **2013**, *184*, 1605–1617.
61. Sjostrand, T.; Mrenna, S.; Skands, P.Z. A Brief Introduction to PYTHIA 8.1. *Comput. Phys. Commun.* **2008**, *178*, 852–867.
62. de Favereau, J.; Delaere, C.; Demin, P.; Giammanco, A.; Lemaître, V.; Mertens, A.; Selvaggi, M. DELPHES 3, A modular framework for fast simulation of a generic collider experiment. *JHEP* **2014**, *2*, 57.
63. Barger, V.D.; Martin, A.D.; Phillips, R.J.N. Sharpening Up the $W \rightarrow t\bar{b}$ Signal. *Phys. Lett. B* **1985**, *151*, 463–468. [[CrossRef](#)]
64. Read, A.L. Presentation of search results: The CL_s technique. *J. Phys. G* **2002**, *28*, 2693. [[CrossRef](#)]
65. Cowan, G.; Cranmer, K.; Gross, E.; Vitells, O. Asymptotic formulae for likelihood-based tests of new physics. *Eur. Phys. J. C* **2011**, *71*, 1–19.

Disclaimer/Publisher’s Note: The statements, opinions and data contained in all publications are solely those of the individual author(s) and contributor(s) and not of MDPI and/or the editor(s). MDPI and/or the editor(s) disclaim responsibility for any injury to people or property resulting from any ideas, methods, instructions or products referred to in the content.